JOURNAL OF SPACECRAFT AND ROCKETS
Vol. 33, No. 2, March–April 1996

Space-Debris Identification Using Optical Calibration of Common Spacecraft Materials

Robert D. Culp* and Ian J. Gravseth†
University of Colorado, Boulder, Colorado 80309

An investigation of the reflective properties of 19 common spacecraft materials was conducted. The experimental setup and the testing procedure are discussed, and a new composite albedo phase function is proposed. Tabular data and graphs of the spectral reflectivities, scattering characteristics, and albedos of these objects are listed for the visible and near infrared wavelengths. Conclusions are drawn regarding the validity of this method, and other possible methods of debris identification are discussed.

Nomenclature

a	= albedo
b	= specular normalization coefficient
c	= exponential estimate
d	= directional scattering normalization coefficient
E	= incident flux
E_r	= reflected flux
f	= directed scattering factor
I	= test object's inclination
R	= radius of sensor
r_A	= radius of illuminated area
β	= proportion of light scattered specularly
γ	= proportion of light scattered diffusely
η	= angle between specular point and reflected light
θ	= phase angle (angle between sensor and incident light)
ρ	= angle between normal vector and reflected light
$1-\beta-\gamma$	= proportion of directionally scattered light

Introduction

DETECTION and measurement of space-debris objects are vital to verify the validity of debris models for low Earth orbit and geosynchronous Earth orbit. Although classically the majority of the debris-object observations are recorded with the use of radars, a large body of growing research suggests that optical observations of debris are an equally valuable tool for debris tracking and cataloging. In fact, some of the work completed by Karl Henize[1,2] suggests that optical instruments may be better suited for detecting some debris objects that are difficult to detect with radar. By measuring optical characteristics of common spacecraft materials, better predictions of the sizes, masses, and material types of the observed debris objects may be obtained. To better understand the optical properties of orbital debris, a detailed study of 19 of the most common materials used in spacecraft construction was conducted.[3] These results will provide estimates of the optical properties of orbiting debris. In turn, these results will allow for researchers to predict the probability of detection of debris fragments of assorted material composition.

Experimental Setup

The experimental setup used in this set of tests was developed and refined during the optical laboratory calibration of the Orbital Debris Radar Calibration Spheres (ODERACS). The testing was conducted in a room specifically designed for optical experiments. The walls, ceiling, and floor of the room were painted black, and the doors to the room sealed to keep out any extraneous light. A large optical table mounted on pneumatic shock absorbers was located at the center of the room, and held the entire testing apparatus.

The testing apparatus consisted of a light source, a secondary mirror, a primary mirror, several light baffles, a circular aperture, a mount for the test articles, and an angular protractor. A detailed diagram of the experimental setup is shown in Fig. 1. The test-object mount was placed at one end of the table, and the primary 16-in. parabolic mirror was placed at the other. The parabolic mirror had a focal length of 88 in. and an angular divergence of approximately 0.5 deg. The light source used in this testing was a 1000-W quartz–halogen light bulb, and it was powered by a constant-current power supply that had a fixed current of 8.0 A. The light emanating from the source was reflected off a secondary mirror and then onto the parabolic mirror, where the collimated beam was sent back down the table so that it illuminated the test articles. A comprehensive set of light baffles was used to shield the test articles from secondary reflections, and a circular aperture of 1-in. diam was placed in the collimated light beam to control the amount of light that illuminated the test articles. The angular protractor held both the test-article mount and a rigid arm that supported the spectrometer's sensor. The readings of the angular protractor could be determined down to tenths of a degree. The test-object mount suspended the observed objects within the collimated light beam, perpendicular to it. The spectrometer used in this experiment had a 512-channel charge-coupled device, with an effective wavelength range of 347.7 to 1056.6 nm. It collected data with a 2-m fiber-optic cable, which was affixed to the sensor's arm.

Experimental Procedure and Data Handling

Each day, before a set of tests was conducted, the alignment of the equipment used in the experiment was checked to help ensure that accurate results were obtained. The light source was turned on and allowed to warm up for at least 15 min before any testing was

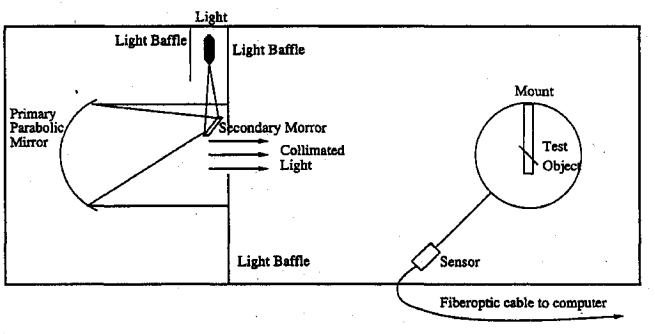

Fig. 1 Basic laboratory setup.

Received April 24, 1995; revision received Nov. 1, 1995; accepted for publication Nov. 13, 1995.

*Professor, Department of Aerospace Engineering, Campus Box 429. Member AIAA.

†Research Assistant, Colorado Center for Astrodynamics, Campus Box 431.

Table 1 Albedo, γ, and β for materials tested

Material	Albedo Mean	Albedo σ	β Mean	β σ	γ Mean	γ σ	c	f	b	d
Aluminum	0.754	0.0970	1.0	—	0	—	—	—	—	—
Lexan®	0.164	0.0810	1.0	—	—	0	—	—	—	—
Kapton®, silver side	0.810	0	1.0	—	0	—	—	—	—	—
Kapton, copper side	0.940	0.0462	1.0	—	0	—	—	—	—	—
Kevlar®	0.679	0.0701	0	—	0.794	0.105	—	1.5	—	0.524
Nextel®	0.724	0.06	0	—	0.9	0.0476	—	3.0	—	0.25
Fiberglass epoxy	0.205	0.0477	0.182	0.0551	0.656	0.183	11.0	3.0	61.0	0.25
Bakelite	0.606	0.0458	0.0676	0.0158	0.9721	0.0561	12.0	3.0	72.5	0.25
Bakelite with parts	0.506	0.0329	0.0263	0.0229	0.981	0.0812	12.0	3.0	72.5	0.25
Silica phenolic	0.188	0.0406	0.280	0.0697	0	—	9.0	2.0	41.0	0.333
Silica phenolic	0.298	0.0094	0.452	0.015	0	—	12.0	2.0	72.5	0.333
Carbon cloth	0.0789	0.0341	0.0765	0.0685	0.823	0.0163	6.0	3.0	18.51	0.25
Carbon epoxy	0.301	0.0581	0.457	0.0865	0	—	5.5	3.0	15.64	0.25
Carbon phenolic	0.172	0.0386	0.0918	0.0628	0.481	0.178	4.0	3.0	8.56	0.25
Carbon phenolic	0.169	0.0340	0.254	0.0563	0	—	15.0	—	113.0	—
Carbon felt insulation	0.0582	0.02	0.928	0.0184	0	—	—	3.0	—	0.25
Nylon	0.519	0.0504	0	—	0.158	0.144	—	1.5	—	0.524
Graphic cloth	0.497	0.102	0.754	0.155	0	—	5.5	1.5	15.64	0.524
MLI 501	0.557	0.0593	0.844	0.0901	0	—	16.0	3.0	128.5	0.25
PCN, white side	0.639	0.0334	0.0674	0.0185	0.932	0.0333	4.0	3.0	8.56	0.25
PCN, black side	0.0875	0.0041	0.219	0.178	0.622	0.185	4.0	3.0	8.56	0.25

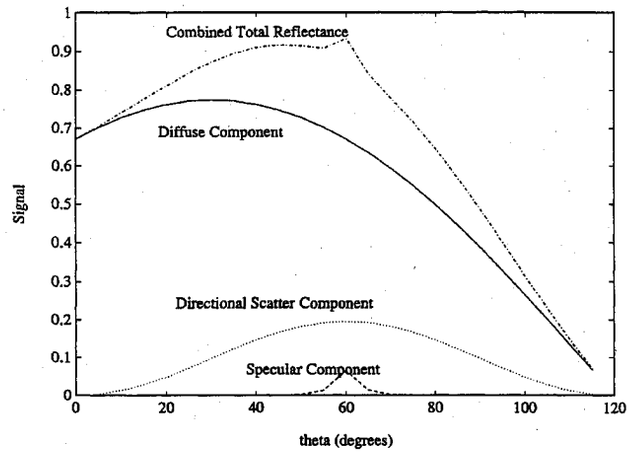

Fig. 2 Individual and combined reflectance terms: I = 30 deg.

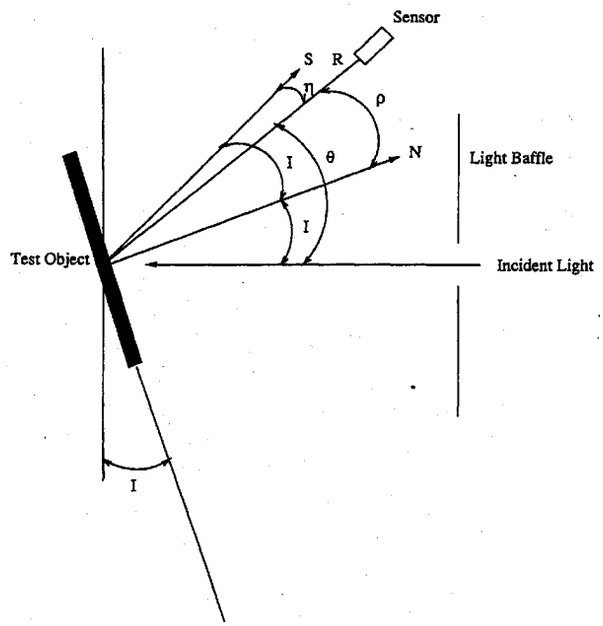

Fig. 3 Angle definitions: N, normal to test object and S, specular point.

undertaken. The test article under examination was then attached to its mount and carefully aligned. Once testing was underway, the reflected spectrum of each sample was recorded every 5 deg in phase angle, except when near the specular point, when measurements were taken every 1 or 2 deg. After every five readings the dark current within the spectrometer was recorded. The direct light signal was recorded immediately before or immediately after a complete set of phase-angle reflectance measurements were recorded. Generally two sets of data were taken on each test article consecutively, and between four and ten sets of data were taken on each surface tested.

After the data were collected on a personal computer, they were transferred to a Sparc II workstation, where they were extensively analyzed.

Analysis of Data

The data were analyzed by two disparate methods. For the highly specular samples, a direct integration method was utilized to obtain the test object's albedo. For the samples where the signal was composed of diffuse, specular, and directional signals, the standard nonlinear goodness-of-fit method was utilized to analyze the data.[4] For each test conducted, the test article's albedo and its β, γ, c, and f coefficients were computed. The final average values for each of these quantities were computed by averaging the results obtained in all reliable tests Standard deviations for each of these quantities were also computed.

Before the reflected signal was analyzed, the dark current was subtracted from each recorded signal, and these results were then

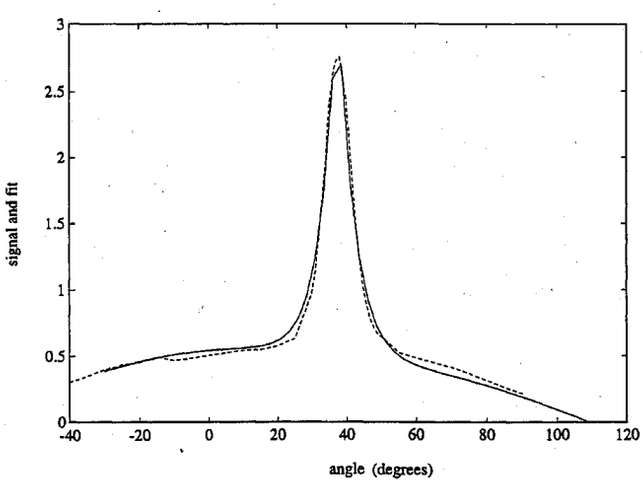

Fig. 4 Least-squares fit and raw data: Bakelite sample: - - -, raw data and —, fit.

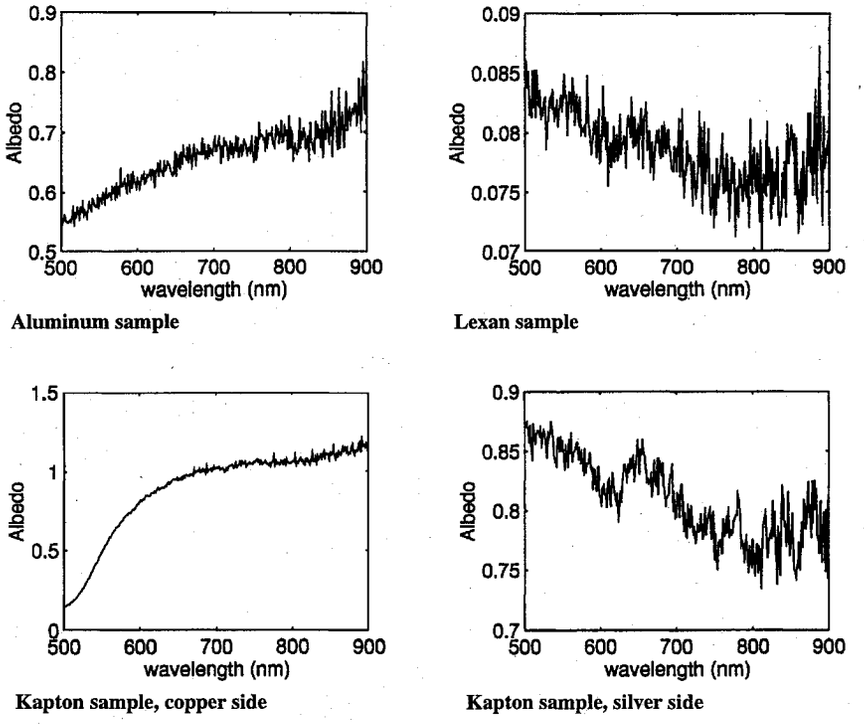

Fig. 5 Albedo vs wavelength: specular samples.

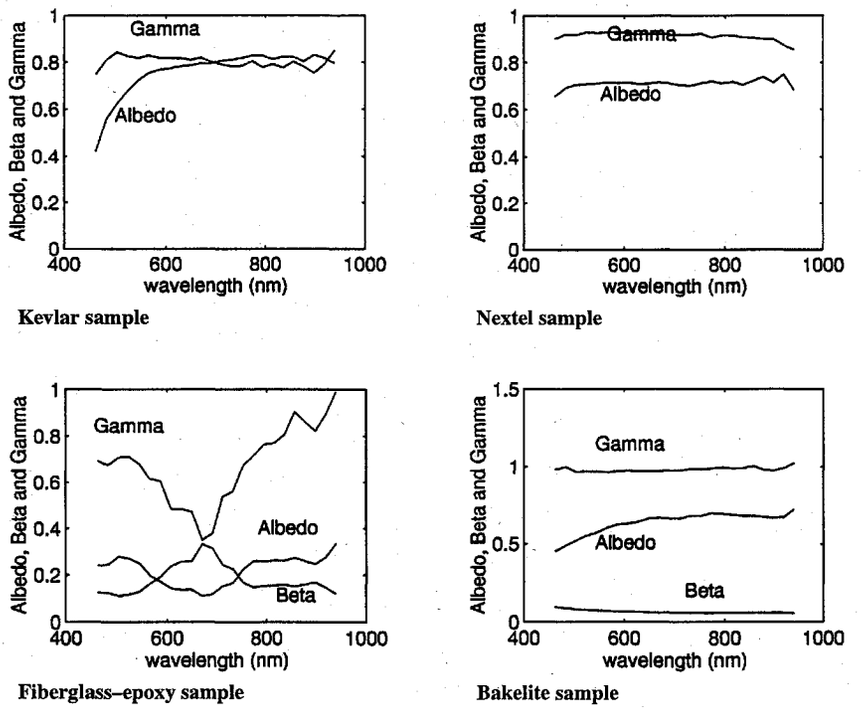

Fig. 6 Albedo, β, and γ vs wavelength: diffuse samples.

normalized by the incident light signal. The numerous experiments conducted with the ODERACS spheres indicated that the dark current within the spectrometer is approximately linear over small time intervals.

The reflected signal was assumed to be composed of the sum of a diffuse and a two-part specular term. Although narrow specular and diffuse terms are common within today's literature, an examination of the reflectance data analyzed revealed that there is in fact a larger spreading in the specular term than was originally thought to have existed. An additional term was added to the data so that the albedo-phase-function equation better modeled the reflected optical data.

The albedo phase function utilized in this analysis is

$$(E_r/E)\cdot\left(R^2/r_A^2\right) = a\cdot[\gamma\cos\rho + \beta b e^{-c\eta} + (1-\beta-\gamma)d(1+\cos f\eta)] \quad (1)$$

$$\rho = |\theta - I| \quad (2)$$

$$\eta = |2I - \theta| \quad (3)$$

Figure 2 shows a graphical representation of the diffuse, highly specular, and directional-scattering terms as well as the composite reflected signal. Figure 3 shows a physical definition of the angular variables listed in the above albedo-phase-function equation.

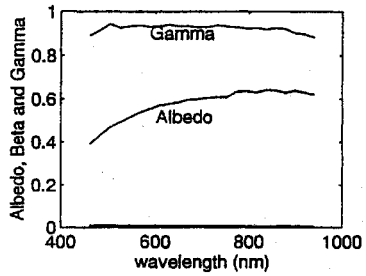

Bakelite with parts sample

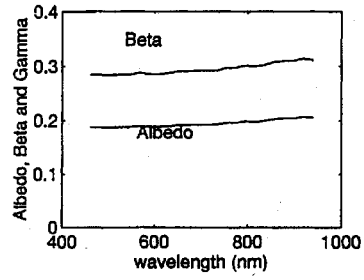

Curved silica phenolic sample

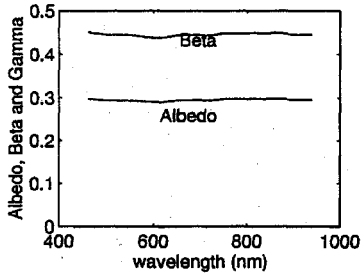

Flat silica phenolic sample

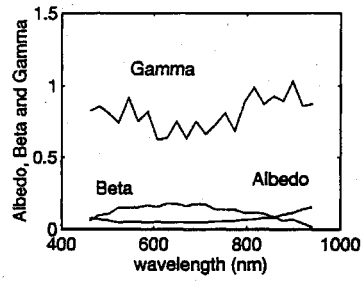

Carbon cloth sample

Fig. 7 Albedo, β, and γ vs wavelength: diffuse samples.

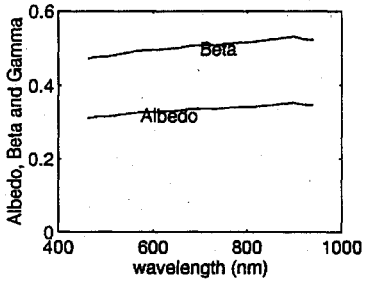

Carbon epoxy sample

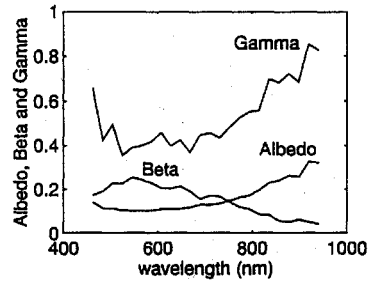

Carbon phenolic sample A

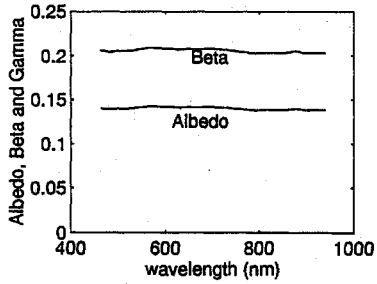

Carbon phenolic sample B

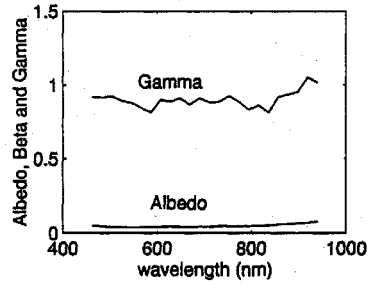

Carbon felt sample

Fig. 8 Albedo, β, and γ vs wavelength: diffuse samples.

Discussion of Results

Table 1 shows a compilation of the results obtained in this study. The values for this table were computed by averaging the albedo, and the coefficients β and γ for all wavelengths within each test and then averaging the results from all tests for each sample. For nearly all the materials tested, no reference albedo values were found. However, the albedo value obtained for the aluminum sample agreed fairly well with the quoted albedo value.[5] Figure 4 gives an example of the raw data and the best-fit signal. Although there are some localized trends within the data that are not modeled in the albedo-phase-function equation, the overall trends within the data are modeled accurately.

Figures 5–10 show a sampling of the albedo and the coefficients β and γ for each of the materials tested over all the analyzed wavelengths. With a few exceptions, most of the materials tested have albedos, and β and γ values that show little variation over the wavelengths tested.

Utilization of These Results

These optical calibrations can be used to obtain predictions of the materials, sizes, and masses of debris particles. Given a set of on-orbit observations, utilizing a least-squares fit or a related approach, the optical constants for any observable piece of debris can be determined. These optical constants can then be compared with the values listed in this paper, and a best guess as to the material composition of the observed object can be made. After a material type is determined, the size of the particle can be computed utilizing flux information from the observations and current albedo information. The mass can then be computed with a mass–characteristic-size equation.[6] Utilizing these results in conjunction with similar

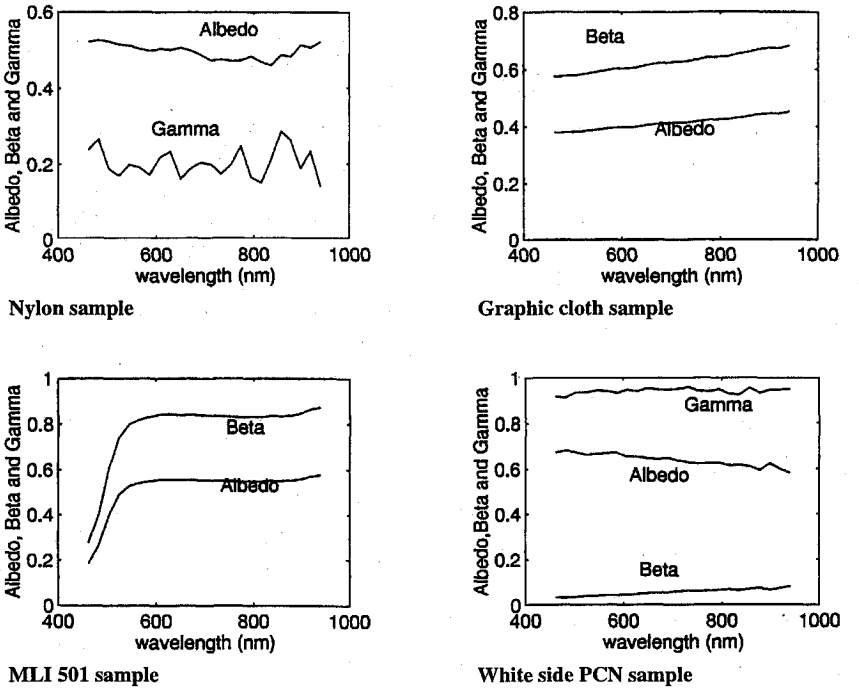

Fig. 9 Albedo, β, and γ vs wavelength: diffuse samples.

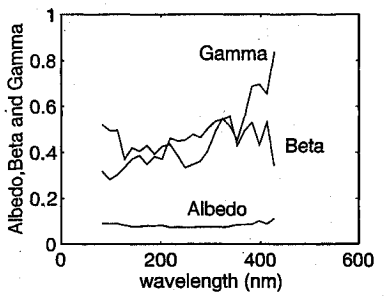

Fig. 10 Albedo, β, and γ vs wavelength—diffuse samples.

observational information from radar, ballistic coefficient, and polarization data should yield more accurate estimates of debris-object sizes and masses.

Conclusions

The methodology and results for the common spacecraft material debris optical testing have been presented. The albedo results for the aluminum test sample agree with published results. Although no published results for the other materials were found, the test results were consistent among themselves and agreed with visual inspection.

Acknowledgments

This study was funded by the NASA Orbital Debris Optical Signature Tests, NGT-50872 and NAG9-407. The authors thank William McClintock of the Laboratory for Atmospheric and Space Physics for the use of his laboratory, equipment, and time. The authors would also like to note that the spectrometer used in this experiment was a Labspec Spectrometer, supplied by Analytical Spectral Devices.

References

[1]Henize, K. G., and Stanley, J., "Optical Observations of Space Debris," AIAA Paper 90-1340, April 1990.

[2]Henize, K. G., Mulrooney, M. K., O'Neill, C. A., and Anz-Meador, P. D., "Optical Properties of Orbital Debris," AIAA Paper 93-0162, Jan. 1993.

[3]Culp, R. D., and Gravseth, I. J., "Optical Calibration of Common Spacecraft Materials," American Astronomical Society, Paper 95-203, Feb. 1995.

[4]Press, W., Flannery, B., Teukolsky, S., and Vetterling, W., *Numerical Recipes*, Cambridge Univ. Press, Cambridge, England, UK, 1989, pp. 521–528.

[5]Anon., *CRC Handbook of Chemistry and Physics*, 62nd ed., CRC Press, Boca Raton, FL, 1981, p. E-386.

[6]Gravseth, I. J., Maclay, T. D., and Culp, R. D., "A Mass–Diameter Function for the Entire Regime of Space Debris," *SPIE Proceedings*, Vol. 2483, April 1995.

A. L. Vampola
Associate Editor